

Propylene Oligomerisation over Ti–Al–Silicalite

Effect of Catalyst Pelleting Pressure

LUCIO FORNI,^{*} MARCO PELOZZI,^{*} ALDO GIUSTI,[†] GIUSEPPE FORNASARI,[†]
AND ROBERTO MILLINI[†]

^{*}*Dipartimento di Chimica Fisica ed Elettrochimica, Università di Milano, Via C. Golgi 19, 20133 Milano, Italy; and* [†]*Eniricerche SPA, Via Maritano 26, 20097 San Donato Milanese, Italy*

Received June 30, 1989; revised October 4, 1989

The nature of diffusion phenomena in Ti–Al–silicalite and ZSM-5 catalysts has been investigated by means of the GC pulse method. Bulk, Knudsen, and intracrystalline contributions to the overall diffusion resistance have been evaluated by employing benzene as a probe molecule. The analysis of these results, together with those coming from a more general physicochemical characterisation of the solid, provide insight into the effect of pelleting pressure on the structure of the catalyst. There are shown to be considerable changes in catalytic activity and aging behaviour in propylene oligomerisation as a function of pelleting pressure. © 1990 Academic Press, Inc.

INTRODUCTION

Preliminary tests of the catalytic activity of some Ti–Al–silicalite-type zeolites for propylene oligomerisation provided evidence that catalyst performance could depend on the pelleting pressure of the solid particles. However, the dependence seemed not to be in line with what one might expect from the usual correlation between pelleting pressure and pore size distribution of the resulting solid, i.e., from the usual effect of diffusional limitation on the overall catalytic process. It seemed then interesting to investigate the reason for such unusual behaviour and to try to determine the nature of the diffusional intrusions in these catalysts.

METHOD

The GC pulse method adopted is described extensively in previous papers (1, 2). The relative importance of the resistance due to the three types of diffusion (bulk, Knudsen, and intracrystalline) on the overall diffusion process may be evaluated from the contribution due to the three types

of diffusion to the parameter C of the van Deemter equation. These parameters are determined from the value of the moments μ'_1 and μ'_2 of the GC peak, which are connected with the height equivalent to the theoretical plate (HETP) of the GC column (1). Particularly, the contribution connected with bulk and Knudsen diffusion may be evaluated from the dependence of the behaviour of the system on the nature of the carrier gas or on the size of solid particles, respectively.

EXPERIMENTAL

Materials. Superpure He (99.9999+ vol%) was employed as carrier gas. It was further purified on precalcined 3A zeolite, maintained at liquid nitrogen temperature, as described previously (1, 2). Analytical-grade hydrocarbons, in most cases benzene (Merck or C. Erba), were used as adsorbate. They were carefully dried on precalcined 3A zeolite spheres and stored on the same desiccant, frequently renewed.

Catalysts. The Ti–Al–ZSM-5 (ER1 and ER3) zeolite samples were prepared as described (3) from mixtures containing tetraethyl orthosilicate, tetrapropylammonium hydroxide (TPAOH), tetraethyl

¹ To whom correspondence should be addressed.

orthotitanate, aluminium isopropoxide, and water at the following molar ratios: $\text{SiO}_2/\text{Al}_2\text{O}_3 = 300$, $\text{SiO}_2/\text{TiO}_2 = 20$, $\text{TPAOH}/\text{SiO}_2 = 0.25$, and $\text{H}_2\text{O}/\text{SiO}_2 = 40$ (ER1) or 10 (ER3). The hydrothermal crystallisation was carried out at 100°C and autogenous pressure for 5 days. The crystalline material was filtered, washed, dried, and calcined in air at 550°C for 5 h.

For comparison sake, an Al-ZSM-5 zeolite sample (ER2) was also prepared according to a Mobil patent (4).

Analysis by the inductively coupled plasma technique (Ti, Al) or by gravimetry (Si) gave the following molar ratios for the main components of the three samples: ER1: $\text{SiO}_2/\text{Al}_2\text{O}_3 = 160$, $\text{SiO}_2/\text{TiO}_2 = 131$; ER2: $\text{SiO}_2/\text{Al}_2\text{O}_3 = 26$; ER3: $\text{SiO}_2/\text{Al}_2\text{O}_3 = 173$, $\text{SiO}_2/\text{TiO}_2 = 120$. The crystalline nature of the samples was checked by XRD, employing $\text{CuK}\alpha$ radiation. ER1 and ER3 showed the typical pentasil-type structure, characterised by the orthorhombic lattice symmetry and unit-cell volume consistent with the presence of both Ti and Al in the silicalite framework. ER2 showed broader reflections, higher degree of line convolution and different relative intensities of the diffraction patterns, due to reduced crystal size or, more likely, to the presence of a defective structure.

Apparatus and procedure. Sorption-diffusion experiments were carried out on the GC pulse apparatus equipped with a U-shaped Pyrex-glass column, described elsewhere (1). Data processing has been speeded up substantially by substituting a bench-top PC, in which an AD converting card was inserted, for the small Epson HX-20 computer employed in the previous work. For the chosen 573 to 623-K temperature range, a short series of preliminary runs showed that the best reliability and reproducibility of data were attained with zeolite bed dimensions of 7–20 cm (length) \times 3 mm (diameter), carrier gas flow rate 20–300 $\text{N cm}^3/\text{min}$ and with injection of less than 0.01 μl of liquid adsorbate.

Catalyst pretreatment and analysis. All

the "as prepared" zeolites showed a marked catalytic activity, due to the presence of their acidic centers. An ion-exchange treatment was therefore needed and this was carried out by means of saturated Na-acetate solution, the pH of which was kept at 10 by adding the proper amount of NaOH. After rapid rinsing in distilled water and drying, the samples were tableted at the desired value of the pressure of pelletting (P_p), gently crushed, and sieved to collect the desired mesh fraction. This was followed by calcination in air overnight at 823 K and heating in He for 6 h at the same temperature. After packing, the GC column was pretreated *in situ* at 773 K for 12 h in a slow flow of dry air, followed by the carrier gas (6 h at the same temperature). Temperature was then lowered to the desired value and the injection of the adsorbate pulses was started. The BET surface area and pore volume distribution have been determined by sorption-desorption of nitrogen at liquid nitrogen temperature or by mercury intrusion. Some selected samples were also examined by SEM and the results are shown in Figs. 1 and 2. The principal characteristics of the columns employed are summarised in Table 1 and in Figure 3.

Catalytic activity tests. Propylene oligomerisation runs were carried out by means of a conventional, continuous, fixed-bed microreactor assembly. Fresh catalyst samples (100 to 500 mg) were employed, diluted with quartz beads to avoid hot spots. Propylene feed (SIAD 99 vol% purity) was diluted (30 vol%) in nitrogen and all the runs were carried out under atmospheric pressure. The reactor effluent was analysed online by GC, employing a 4.5-m-long Porapak QS column.

RESULTS AND DISCUSSION

Catalytic Tests

Effect of particle size. The sensitivity of the catalysts to internal diffusion in propylene oligomerisation was tested on samples of different particle sizes. ER1(5) was

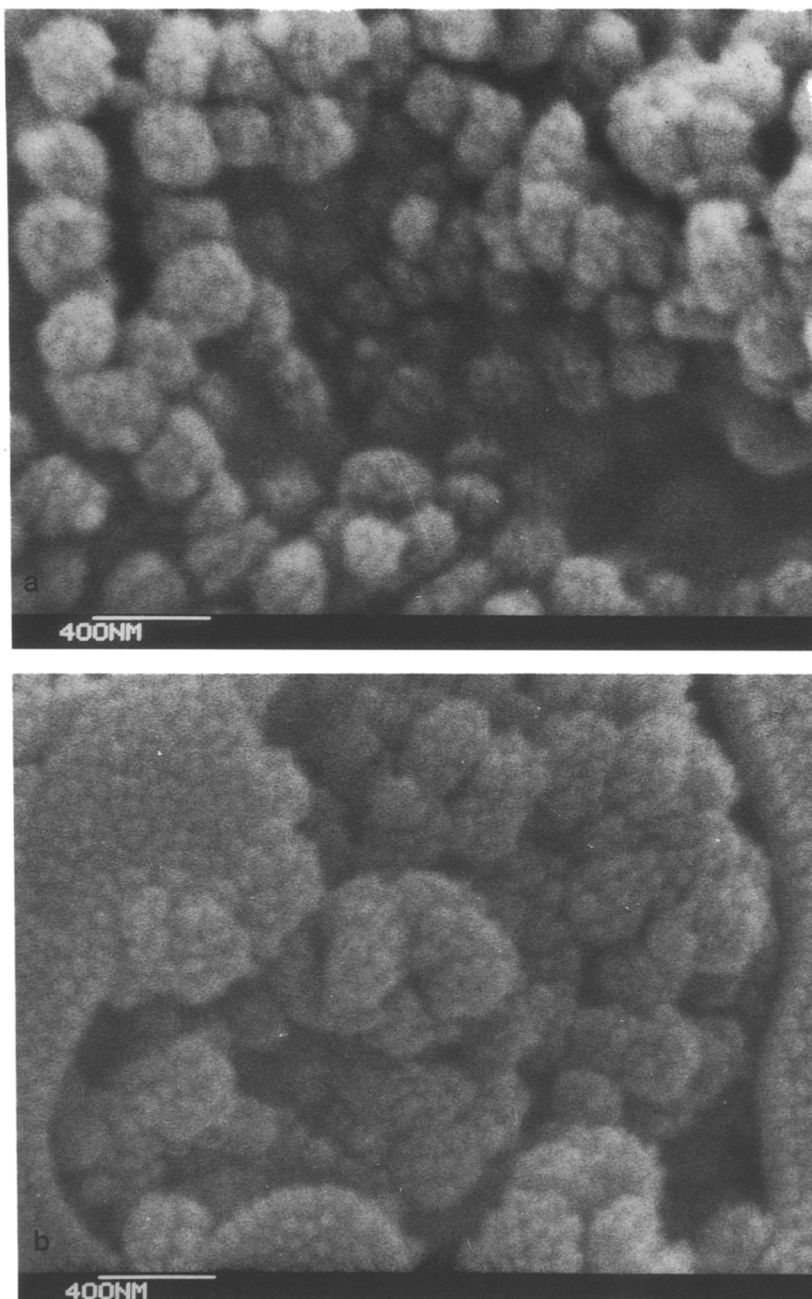


FIG. 1. Typical SEM micrographs of (a) ER1(0), (b) ER1(5)B, and (c) ER1(10)B samples. For symbolism, see text and Table 1.

crushed and sieved to granules with average diameters of 0.60, 0.95, and 1.50 mm, respectively. Another sample of ER1 was bound with alumina (1:1 by weight), pel-

leted at 5 tons, crushed, and sieved to the same particle sizes.

The oligomerisation reaction was carried out at 551 K, C_3H_6 partial pressure of 0.14

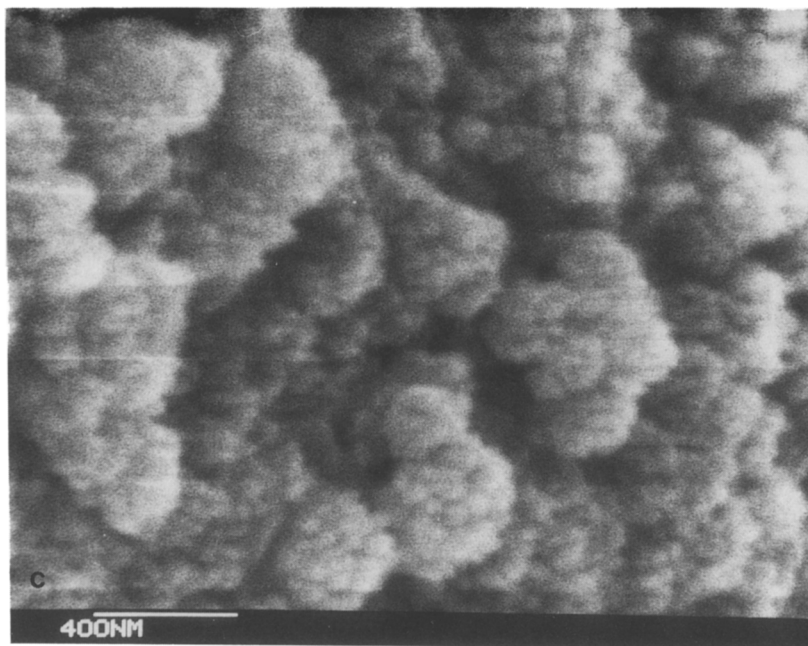


FIG. 1—Continued

$\times 10^5$ Pa and 24 h^{-1} WHSV. The results, expressed as conversion of propylene vs time-on-stream up to 60 h, are given in Figs. 4 and 5 for unbound and bound sets of samples, respectively.

In both cases the initial activity appears to be inversely related to particle size, confirming the presence of internal diffusion phenomena. For the unbound samples (Fig. 4) the diffusive limitation is more evident and a dependence of aging on particle size can also be observed. The mean values of the angular coefficient of the decay curves, obtained by regression on the experimental points, are collected in Table 2. Since an increasing diffusion limitation of product release can be related directly to faster aging of the catalyst, it may be concluded that both reactants and products are involved in diffusion phenomena when ER1 is used as catalyst.

Alumina-bound samples behave in a qualitatively similar way (Fig. 5), although the effect on initial activity and aging seems

slightly reduced by the presence of the diluting material.

The particle size effect under identical conditions was studied also on ER2(5) catalyst. Figure 6 shows the results. In this case a decrease in initial conversion of propylene may be observed only for the largest particles, but the deactivation behaviour seems to be independent of particle size (Table 2). This indicates less influence of internal diffusion on this catalyst. The lower activity of the largest particles can be related to the increasing influence of the bypassing phenomenon of the reactant through the bed of catalyst. This phenomenon has less influence on aging.

Effect of pelleting pressure. The influence of the pressure of pelleting on catalytic performance has been studied on three samples of ER1 zeolite, bound with alumina (50% by weight), pelleted at 1, 5, and 10 tons/cm², respectively, crushed and sieved to 20–40 mesh (0.84–0.42 mm). Reaction conditions were 551 K, C₃H₆ partial

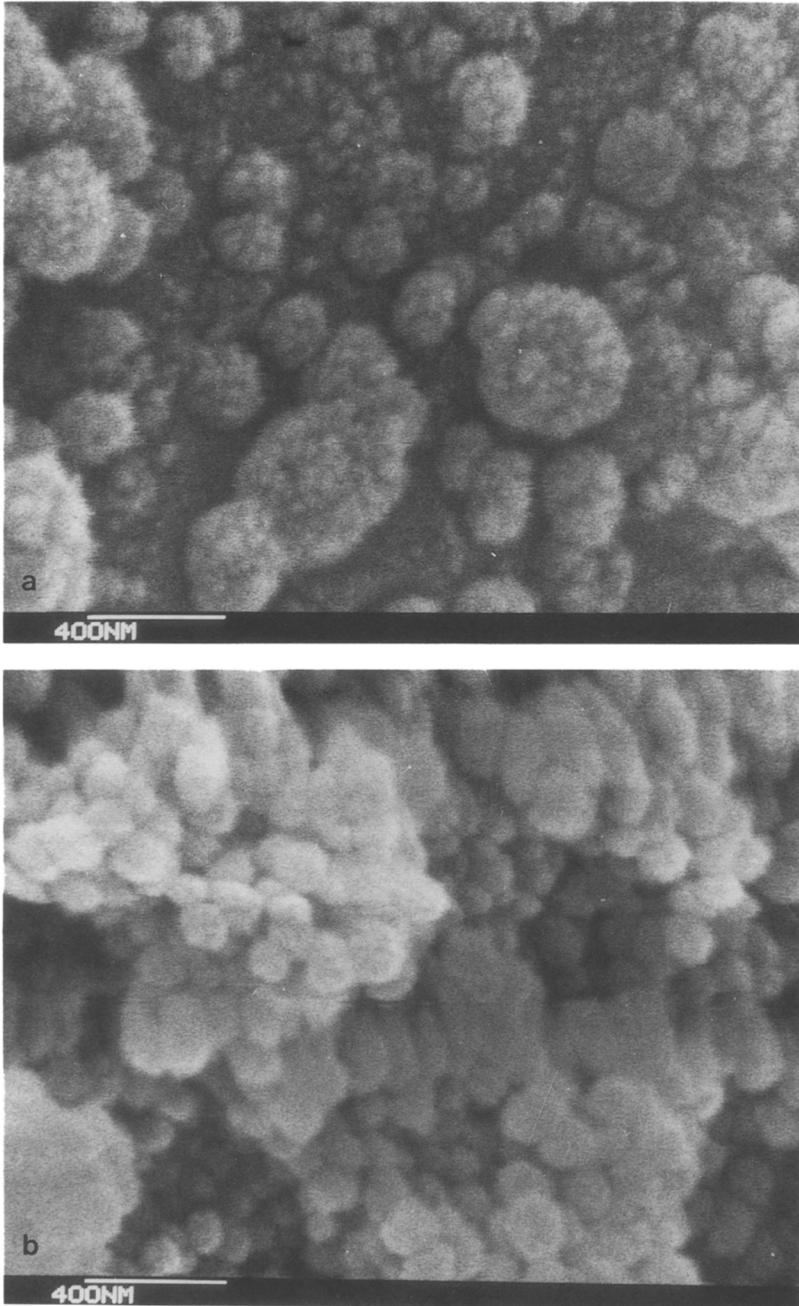


FIG. 2. Typical SEM micrographs of (a) ER2(0) and (b) ER3(0) samples.

pressure 0.14×10^5 Pa, and WHSV of about 24 h^{-1} . The results are collected in Fig. 7. All the samples show an 80–85% initial con-

version level, that pressed at 5 tons appearing to be the most active and that pressed at 10 tons the least active. This unusual be-

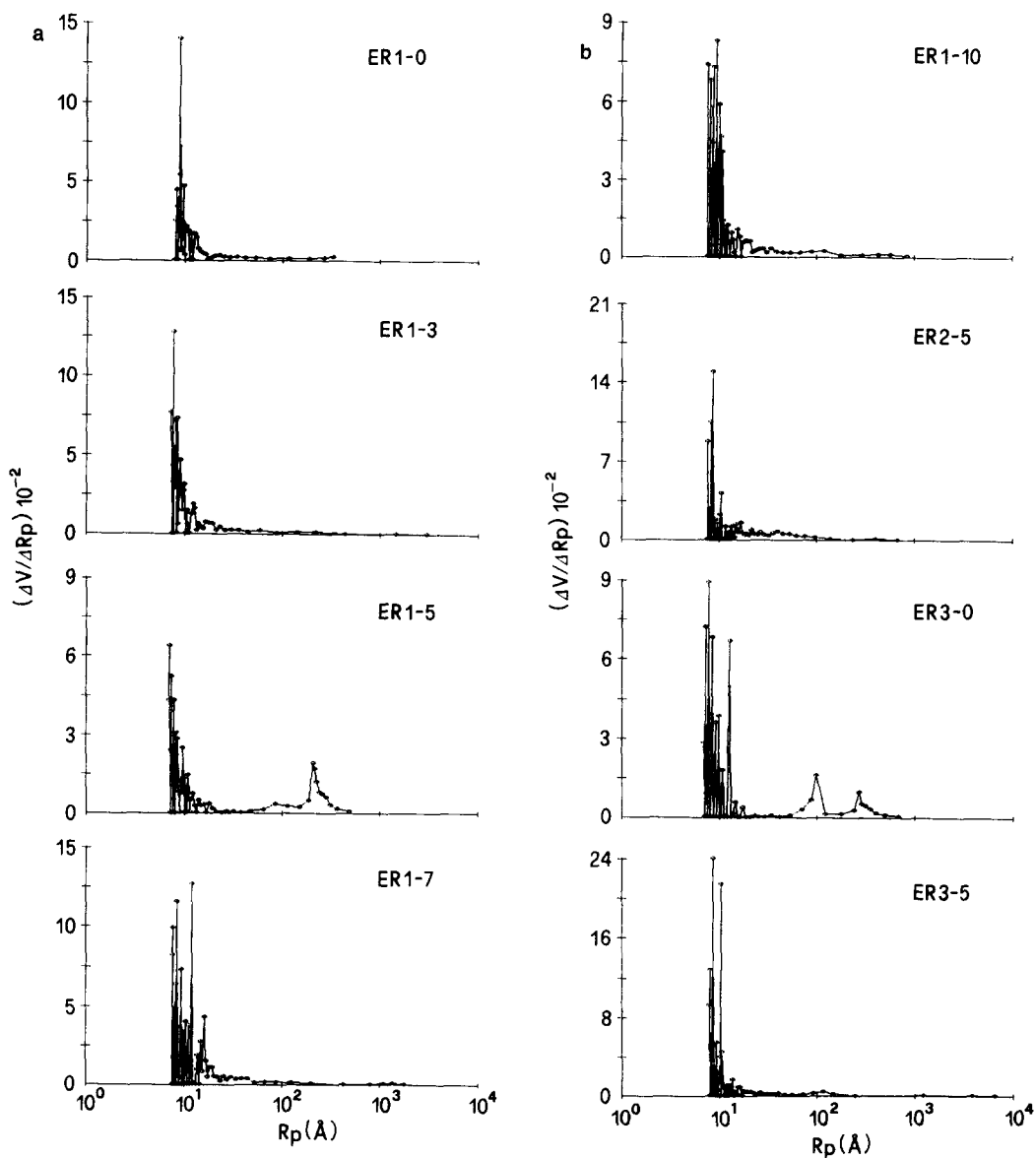


FIG. 3. Pore volume distribution of samples listed in Table 1.

haviour follows the same trend of porosity vs the same parameter P_p (see Fig. 3 and Table 1, last column).

By following the propylene conversion vs time-on-stream one can observe that all three catalysts age quite slowly, the aging being more evident for the sample pressed at 10 tons. The performance of the sample

pressed at 1 ton seems better: while starting at a slightly lower level with respect to the sample pressed at 5 tons, after ca. 30 h on stream it attains the best performance of the group. Practically no difference in selectivity, both with fresh and aged catalyst, was noted for the three samples, as shown in Table 3.

TABLE 1

| Characteristics of the GC Columns Employed | | | | |
|--|--------------------|----------------|------------------------------|-------------------------------|
| Column ^a | Column length (cm) | Bed weight (g) | BET s.a. (m ² /g) | Pore vol (cm ³ /g) |
| ER1(0) ^b | — | — | 577 | 0.6 (0.7) ^c |
| ER1(2)A | 9.6 | 0.338 | | |
| ER1(2)B | 7.0 | 0.252 | | |
| ER1(2)C | 8.7 | 0.297 | | |
| ER1(3)A | 11.6 | 0.422 | 501 | 0.9 |
| ER1(3)B | 9.6 | 0.359 | | |
| ER1(3)C | 8.0 | 0.299 | | |
| ER1(5)A | 11.7 | 0.498 | 483 | 1.7 (1.6) ^c |
| ER1(5)B | 10.4 | 0.401 | | |
| ER1(5)C | 11.1 | 0.466 | | |
| ER1(7)A | 11.4 | 0.480 | 369 | 1.1 |
| ER1(7)B | 10.5 | 0.442 | | |
| ER1(7)C | 9.4 | 0.416 | | |
| ER1(10)A | 11.8 | 0.543 | 425 | 0.9 (0.9) ^c |
| ER1(10)B | 8.2 | 0.322 | | |
| ER1(10)C | 7.2 | 0.251 | | |
| ER2(5)A ^d | 10.7 | 0.352 | 362 | 0.8 |
| ER2(5)B | 8.4 | 0.294 | | |
| ER2(5)C | 8.1 | 0.279 | | |
| ER3(0) | — | — | 574 | 1.5 |
| ER3(5)A | 12.5 | 0.474 | 537 | 1.0 |
| ER3(5)B | 11.2 | 0.419 | | |
| ER3(5)C | 10.2 | 0.400 | | |

Note. External void fraction $\epsilon = 0.49$ – 0.50 for all the columns.

^a Digits in parentheses represent the value of P_p (t/cm²). A, B, and C represent the average particle size: A = 0.031, B = 0.020, C = 0.016 cm; the absence of this final letter indicates the original unpelleted powder cake.

^b Average size of zeolitic crystals 2×10^{-6} cm.

^c Duplicated data (see text).

^d Average size of zeolitic crystals 3×10^{-6} cm.

Effect of Pelleting Pressure on Diffusive Behaviour

The effect on the diffusive behaviour within the samples of changing the value of P_p has been studied by employing benzene instead of propylene, so that temperatures

TABLE 2

Average Angular Coefficient of the Decay Curve

| Catalyst | Particle size (mm) | | |
|----------|--------------------|----------|---------|
| | 0.42–0.85 | 0.85–1.0 | 1.0–2.0 |
| ER1(5) | -0.168 | -0.231 | -0.234 |
| ER2(5) | -0.214 | — | -0.219 |

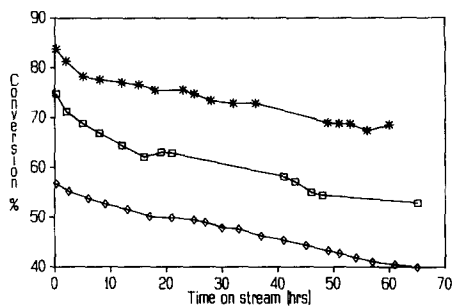


FIG. 4. Effect of catalyst particle size on conversion. ER1(5) catalyst, 551 K, 24 h⁻¹ propylene WHSV, and 0.14×10^5 Pa feed partial pressure. Particle size (mm): (*) 0.42–0.85, (□) 0.85–1.0, and (◇) 1.0–2.0.

corresponding to the usual working conditions of these zeolites as catalysts could be attained in the absence of any reaction, due to the particular stability of the aromatic molecule. The 573- to 623-K temperature range was chosen. Experimental results have been expressed in terms of C_b , C_k , and C_i , i.e., the contributions to the van Deemter parameter C due to bulk, Knudsen, and intracrystalline diffusion, respectively. Furthermore, since the change of P_p affects chiefly the intraparticle–intercrystalline diffusion, which is essentially of the Knudsen type, the value of the apparent Knudsen diffusion coefficient D_k was also calculated. The experimental data are collected in Table 4.

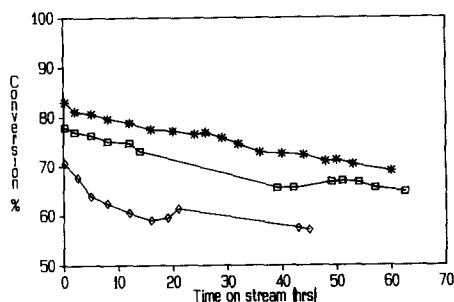


FIG. 5. Effect of catalyst particle size on conversion. ER1 + Al₂O₃ (1:1 by weight) catalyst, pelleted at 5 tons/cm². Reaction conditions and symbols as for Fig. 4.

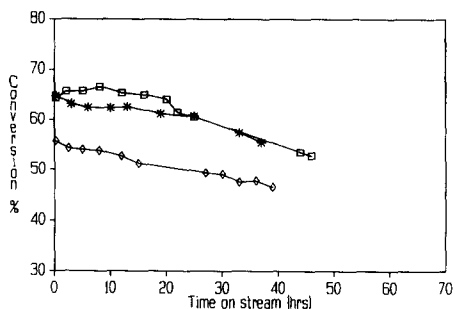


FIG. 6. Effect of catalyst particle size on conversion. ER2(5) catalyst. Reaction conditions and symbols as for Fig. 4.

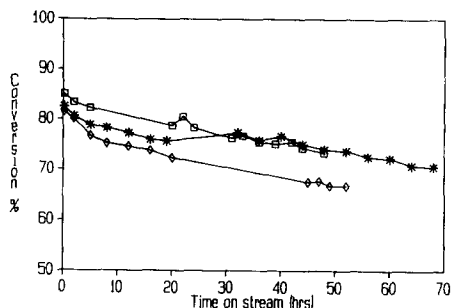


FIG. 7. Effect of catalyst pelleting pressure on conversion. ER1 + Al₂O₃ (1 : 1 by weight) catalyst. Reaction conditions as for Fig. 4. P_p (t/cm²): (*) 1, (□) 5, and (◇) 10.

A careful analysis of the whole set of data relative to ER1 zeolite, by taking into account that the higher the value of the parameter C_j , the more important is the j th diffusion phenomenon, allows one to make the following observations.

(i) The contribution due to bulk diffusion depends only on temperature and on external void fraction ϵ of the GC column. Hence, besides temperature, it must be a function of the particle size only. Indeed, it decreases, as expected, both with increasing temperature and with decreasing particle size. The value of C_b was completely independent of P_p and lower than both C_k and C_i , by ca. one order of magnitude. This means that, for each column, bulk diffusion

contributes by no more than 10% to the overall diffusive resistance. We suggest that this type of diffusion, besides occurring within the interparticle voids, very probably takes place also in the intraparticle voids existing between the berry-like conglomerates of zeolitic crystals, shown by SEM micrographs (Figs. 1 and 2).

(ii) The contribution due to Knudsen diffusion depends strongly on P_p . The relative importance of this type of diffusion increases on going from $P_p = 2$ to 5 t/cm² and then decreases for higher values of P_p . We suggest that this type of diffusion very probably takes place essentially within the intercrystalline-intraparticle voids existing within the "seeds" of the berry-like con-

TABLE 3
Selectivity to Oligomerisation Products

| P_p (t/cm ²) | Time on stream (h) | % Selectivity to | | | | | | | | |
|-------------------------------|--------------------------|------------------|-------|-------|-------|-------|-------|-------|-------|-------|
| | | C_1 | C_2 | C_3 | C_4 | C_5 | C_6 | C_7 | C_8 | C_9 |
| 1 | 0.2 | 0 | 0.05 | 0.5 | 30.7 | 29.1 | 17.9 | 12.9 | 8.9 | Tr |
| | 60 | 0 | 0.04 | 0.4 | 31.4 | 28.0 | 18.2 | 12.9 | 7.8 | 1.2 |
| 5 | 0.2 | 0 | 0.05 | 0.5 | 30.7 | 29.9 | 18.8 | 12.5 | 7.5 | Tr |
| | 46 | 0 | 0.03 | 0.4 | 30.6 | 28.4 | 18.4 | 13.0 | 8.0 | 1.2 |
| 10 | 0.2 | 0 | 0.05 | 0.5 | 31.8 | 29.3 | 18.3 | 12.5 | 7.6 | Tr |
| | 52 | 0 | 0.03 | 0 | 30.5 | 27.0 | 18.8 | 13.5 | 8.7 | 1.5 |

Note. ER1 + Al₂O₃ (1 : 1 by weight) catalyst.

TABLE 4
Sorption-Diffusion Experimental Data (Adsorbate: Benzene)

| Column | $10^4 \times C_b(s)^a$ | | | $10^4 \times C_k(s)$ | | | $10^4 \times C_i(s)$ | | | $D_k(\text{cm}^2/\text{s})^b$ | | | |
|----------|------------------------|-------|-------|----------------------|-------|-------|----------------------|-------|-------|-------------------------------|-------|-------|-------|
| | 573 K | 598 K | 623 K | 573 K | 598 K | 623 K | 573 K | 598 K | 623 K | 573 K | 598 K | 623 K | |
| ER1(2)A | | | | | 8.09 | | | 13.3 | | | | 0.154 | |
| ER1(2)B | | | | | 3.37 | | | 11.6 | | | | | |
| ER1(2)C | | | | | 2.07 | | | 11.4 | | | | | |
| ER1(3)A | | | | | 9.26 | | | 9.83 | | | | 0.144 | |
| ER1(3)B | | | | | 3.85 | | | 12.2 | | | | | |
| ER1(3)C | | | | | 2.25 | | | 10.7 | | | | | |
| ER1(5)A | 2.46 | 2.28 | 2.12 | 14.3 | 14.0 | 13.7 | 1.09 | 2.74 | 5.55 | 0.087 | 0.089 | 0.091 | |
| ER1(5)B | 1.02 | 0.95 | 0.88 | 5.95 | 5.83 | 5.71 | 3.43 | 5.00 | 6.31 | | | | |
| ER1(5)C | 0.63 | 0.59 | 0.55 | 3.67 | 3.59 | 3.52 | 2.69 | 3.56 | 3.88 | | | | |
| ER1(7)A | | | | | 8.57 | | | 5.39 | | | | 0.147 | |
| ER1(7)B | | | | | 3.57 | | | 5.32 | | | | | |
| ER1(7)C | | | | | 2.20 | | | 5.45 | | | | | |
| ER1(10)A | | | | | 2.44 | | | 15.1 | | | | 0.511 | |
| ER1(10)B | | | | | 1.02 | | | 15.2 | | | | | |
| ER1(10)C | | | | | 0.63 | | | 15.2 | | | | | |
| ER2(5)A | | | | | 10.0 | 9.82 | | 20.9 | 18.2 | | | 0.125 | 0.127 |
| ER2(5)B | | | | | 4.17 | 4.09 | | 24.7 | 15.4 | | | | |
| ER2(5)C | | | | | 2.57 | 2.52 | | 22.1 | 17.4 | | | | |
| ER3(5)A | | | | | 6.11 | | | 11.5 | | | | 0.206 | |
| ER3(5)B | | | | | 2.54 | | | 12.5 | | | | | |
| ER3(5)C | | | | | 1.57 | | | 12.2 | | | | | |

Note. Average standard deviations: $\pm 5\%$ for C_k and C_i , $\pm 10\%$ for C_b . D_k calculated by assuming $\tau/\theta \cong 4$, τ being the tortuosity factor and θ the internal particle void fraction (see Ref. (5)).

^a As C_b is independent of pelleting pressure, it has been reported only for the intermediate value (5 t/cm^2) of this parameter.

^b D_k is independent of particle size, so it has the same value for each A, B, C set of columns.

glomerates, the seeds being the zeolitic microcrystals sticking together to form the conglomerate.

The analysis by SEM is perfectly in line with this suggestion. Indeed, the sequence of micrographs (Figs. 1a, 1b, and 1c) referring to ER1(0), ER1(5), and ER1(10) samples, respectively, shows clearly that the berries present in the original, unpelleted ER1(0) material, on pressing up to $P_p = 5 \text{ t/cm}^2$ tend to stick together to form much larger conglomerates. As a consequence, in the ER1(5) particles diffusion between the seeds must take place through a much longer path with respect to the original ER1(0) berries. By further increasing P_p the larger conglomerates break up again into smaller ones (Fig. 1c), whose average diameter is of the same order of magnitude as the original ER1(0) berries. As a consequence, the length of the Knudsen diffusive path reduces again. Furthermore, as ex-

pected, the value of C_k decreases both with increasing temperature and with decreasing particle size.

(iii) The relative importance of the contribution due to intracrystalline diffusion as a function of P_p shows a trend practically opposite to that due to Knudsen diffusion. Following the previous suggestion, this type of diffusion probably takes place within the seeds of the berry-like conglomerates, i.e., within the channels of the zeolitic crystals. The relative values of C_i and C_k show that, with the present material and in the explored range of experimental conditions, intracrystalline and Knudsen diffusions play a competitive but comparable role, except for the lowest ($\leq 3 \text{ t/cm}^2$) or the highest (10 t/cm^2) values of P_p . Furthermore, as expected, C_i increases considerably with increasing temperature and, due to the competition of the Knudsen-type diffusion, it increases and then decreases on go-

ing from the larger (0.031 cm) to the medium-size (0.020 cm) to the smaller (0.016 cm) particles.

In any case, as expected, the strongest dependence on P_p of the diffusive behaviour of the adsorbate is shown by the Knudsen-type diffusion, since usually the crystalline structure withstands the pressure forces much better than the structure of a simple conglomerate of microcrystals.

As for the ER2 and ER3 samples, our data show that for both these zeolites a pelleting pressure of 5 t/cm² never leads to the prevailing of the Knudsen-type diffusion resistance, C_k being always lower than C_i by ca. one order of magnitude.

A further confirmation of the effect of P_p on ER1 zeolite comes from the BET surface area and porosity data (Table 1 and Figure 3). By increasing P_p up to 5 t/cm² the surface area decreases from 577 to 483 m²/g and a group of mesopores forms, with mean radius of ca. 20 nm, while the overall pore volume progressively grows from ca. 0.6 to ca. 1.7 cm³/g. These mesopores disappear by further increasing P_p and the surface area goes through a minimum at $P_p = 7$ t/cm², the pore volume decreasing again, reaching ca. 0.9 cm³/g at $P_p = 10$ t/cm². In addition, by comparing the distribution of pore volume as a function of pore radius (Fig. 3), it may be seen that the change in overall porosity is simply connected with

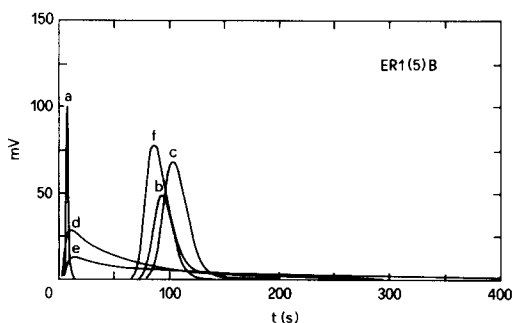


FIG. 8. Sorption-desorption behaviour of some adsorbates on the ER1(5)B column. (a to f) Ethane, benzene, toluene, *o*-, *m*-, and *p*-xylene, respectively.

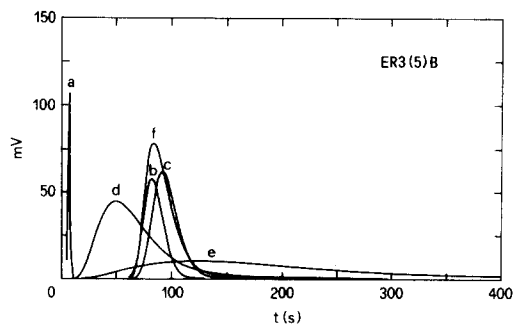


FIG. 9. As for Fig. 8, but for the ER3(5)B column.

the formation or disappearing of the above mentioned mesopores, the original amount of pore volume, due to the zeolitic micropores, remaining practically unchanged. At first sight this behaviour was quite surprising. However, a duplication of some selected data confirmed the previous trend (last column of Table 1).

A different behaviour has been observed with the ER3 sample, for which pressing to $P_p = 5$ t/cm² gave a much smaller change in surface area (from 574 to 537 m²/g) and a decrease instead of an increase in pore volume, together with disappearance of the original pore volume connected with the 10- to 30-nm pores.

Some qualitative experiments under identical conditions were then carried out, by simply comparing the residence time and the shape of the elution peak of some selected adsorbates on the ER1(5)B and ER3(5)B columns, aiming at collecting some additional information about this different behaviour. The results are shown in Figs. 8 and 9. It may be seen that, as expected, due to the inertness of the paraffinic species, ethane does not adsorb appreciably, the retention time practically corresponding to the residence time of the carrier gas. Benzene, toluene, and *p*-xylene adsorb and diffuse similarly, while *o*- and *m*-xylene diffuse much more slowly and mostly bypass the bed without adsorbing, as shown by the rapid elution of most of the injected sample. However, some difference can be noted in the retention time of the

same adsorbate through the two columns, indicating that the ER3(5) pore system allows an appreciably faster sorption-diffusion of the various adsorbates. In our opinion this should be attributed to a slightly larger diameter of the ER3 zeolitic channels more than to a lesser influence of the Knudsen-type diffusion resistance (see Table 4 data, referring to the values of C_i and C_k for the two columns).

It must be remembered, however, that a direct comparison of the C_j data relative to different solid samples should not be made in general or when comparing data collected under identical conditions. This is because C_j data express only the relative importance of the three diffusive phenomena of a given sample. They do not express the absolute value of the three diffusive resistances. Furthermore, it may be easily noted that the relative importance of the three diffusive phenomena changes markedly with changing of the experimental conditions or the conditions of pretreatment of the solid, because of the well-known fact that the resistance due to bulk diffusion grows when the particle size is increased, while that of the intracrystalline diffusion grows when the zeolitic crystal size is increased, and, finally, that of Knudsen diffusion grows when the size of the intragranular-intercrystalline voids is decreased.

To sum up, the comparison of the diffusive behaviour of different adsorbates in different porous materials should always be made on the basis of a large set of data, including porosity, size of particles, of crystals, and of crystalline conglomerates, and, last but not least, the elution rate of the adsorbates.

CONCLUSIONS

Even pelleting, apparently the simplest operation among those carried out during

the preparation of a zeolite-based catalyst, seems far from being trouble-free. When the powdered material is subjected to increasing pressure, it may undergo significant structural changes. This can bring about a considerable variation in the relative importance of the various types of diffusion, especially Knudsen and intracrystalline diffusion, taking place within the pellet during the catalytic reaction.

In the present case, the unusual trend of activity vs pelleting pressure (see, e.g., the data in Fig. 7) has been found to be due probably to the formation and disappearance of different-sized conglomerates of microcrystals. The size of the latter is likely to be one of the most important features governing the phenomenon. Indeed, when the intercrystalline-intraparticle voids, i.e., the locus where the Knudsen diffusion principally takes place, are of the proper size, a competition may arise between intraparticle and intracrystalline diffusion resistance. This can lead to a considerable change in catalytic behaviour as a function of pelleting pressure, connected with the relative length of the path that reactants and products must go through under competitive diffusion restrictions.

ACKNOWLEDGMENTS

Thanks are due to Dr. S. Csicsery for stimulating discussions. Eniricerche is indebted to AGIP SpA for supporting this research.

REFERENCES

1. Forni, L., Viscardi, C. F., and Oliva, C., *J. Catal.* **97**, 469 (1986).
2. Forni, L., and Viscardi, C. F., *J. Catal.* **97**, 480 (1986).
3. Italian Patent 23291A/85, Dec. 1985.
4. British Patent 1402981, Jan. 1984.
5. Satterfield, C. N., "Mass Transfer in Heterogeneous Catalysis," Chap 1. MIT Press, Cambridge, MA, 1970.